Chemistry & Biology, Vol. 9, 707–712, June, 2002, ©2002 Elsevier Science Ltd. All rights reserved. PII S1074-5521(02)00151-5

Structure of TAR RNA Complexed with a Tat-TAR Interaction Nanomolar Inhibitor that Was Identified by Computational Screening

Zhihua Du, Kenneth E. Lind,[2] and Thomas L. James[1]
Department of Pharmaceutical Chemistry
University of California, San Francisco
San Franciso, California 94143

Summary

HIV-1 TAR RNA functions critically in viral replication by binding the transactivating regulatory protein Tat. We recently identified several compounds that experimentally inhibit the Tat-TAR interaction completely at a 100 nM concentration. We used computational screening of the 181,000-compound Available Chemicals Directory against the three-dimensional structure of TAR [1]. Here we report the NMR-derived structure of TAR complexed with acetylpromazine. This structure represents a new class of compounds with good bioavailability and low toxicity that bind with high affinity to TAR. NMR data unambiguously show that acetylpromazine binds only to the unique 5′ bulge site to which the Tat protein binds. Specificity and affinity of binding are conferred primarily by a network of base stacking and hydrophobic interactions. Acetylpromazine alters the structure of free TAR less than Tat peptides and neomycin do.

Introduction

The past decade has witnessed rapid progress in the structure determination of biologically important RNA molecules via X-ray crystallography and NMR. The newly available structural information not only provides valuable insights into how RNA molecules function in living cells but also opens the avenue for discovery of RNA-targeting therapeutic agents based on the detailed three-dimensional structure. We have demonstrated the feasibility of our structure-based computational screening strategy for drug discovery. We have identified several small-molecular-weight organic compounds that bind HIV-1 TAR and completely inhibit, at concentrations of 100 nM, its interaction with equimolar HIV-1 Tat protein [1, 2].

The TAR-Tat protein interaction is essential for HIV replication because the binding of Tat to TAR is required for activating transcription of the HIV genome [3, 4]. Finding therapeutic agents that disrupt the Tat-TAR interaction therefore would provide a strategy for inhibiting HIV replication. Based on an NMR-derived structural model of HIV-1 TAR, we have performed computational virtual screening of the approximately 153,000–181,000 compounds in the Available Chemicals Directory (ACD) [1, 2]. Using NMR as an experimental screening tool, we have verified that some of the top-scoring compounds identified via virtual screening actually bind to the 5′ bulge of TAR (see Figure 1A for a secondary-structure diagram of HIV-1 TAR) in solution. The 5′ bulge is the same region previously identified as the site of Tat binding [5–7]. We have also shown via electrophoretic mobility shift assays that these TAR ligands, at concentrations between 0.1 and 1 μM, disrupt the Tat-TAR interaction in vitro [1]. In the current paper, we present the high-resolution NMR structure of TAR in complex with acetylpromazine (also known as acetopromazine or acepromazine; see Figure 1B for the chemical structure). At a concentration of 100 nM, acetylpromazine completely inhibited the interaction of TAR and Tat, both at 100 nM. While the acetylpromazine-TAR structure is largely consistent with that predicted in our computational screen, the experimentally determined structure shows that the conformation of the target TAR is modified somewhat upon complex formation. Using the structure of the complex, we can suggest ways likely to improve binding affinity and specificity in the next cycle of drug design and development in particular and to provide insights into RNA structure-based drug discovery in general.

Results and Discussion

Specific Binding of Acetylpromazine to the TAR Internal Bulge

One-dimensional imino proton spectra in Figure 2A show selective changes in chemical shifts as acetylpromazine is added to free TAR and confirm that a 1:1 complex is formed. Some of the signals are broadened more than one would expect from the gain in size, implying that complex formation occurs in the intermediate exchange regime of the NMR time scale.

Within HIV-1 TAR, the Tat binding site comprises the 5′ bulge with three pyrimidine residues, U23, C24, and U25 (Figure 1A), and their adjacent base-pairs. Because these and other pyrimidine residues yield distinctive H5-H6 crosspeaks in a 2D TOCSY spectrum, we have been able to use homonuclear 2D TOCSY experiments to identify compounds that bind to the 5′ bulge by examining chemical-shift changes in the H5-H6 region [1]. We have shown that upon addition of acetylpromazine, only those pyrimidine residues in the bulge region (U23, C24, U25, C39, and U40) exhibited noticeable chemical-shift changes, whereas other pyrimidine residues were not affected. This dramatic result provided the first line of NMR evidence indicating that acetylpromazine interacted with TAR specifically in the bulge region. Subsequent heteronuclear NMR experiments performed on various labeled TAR samples confirmed that all of the observed chemical-shift changes induced by acetylpromazine were confined to residues within or around the 5′ bulge (reference [1] and Figures 2B–2D herein). Numerous spectral assignments for TAR, both free and in the presence of acetylpromazine at a ratio of 2:1, enabled us to readily identify the following substantial (>0.1 ppm) proton chemical-shift changes (downfield and upfield shifts are denoted by positive and negative

[1]Correspondence: james@picasso.ucsf.edu
[2]Present Address: Structural GenomiX, 525 Brannan St., Suite 200, San Francisco, CA 94107.

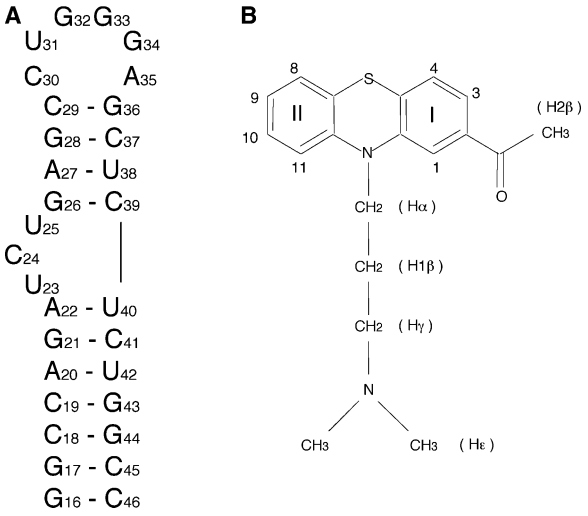

Figure 1. HIV-1 TAR RNA and Acetylpromazine

(A) Sequence and numbering system of the 31 nucleotide HIV-1 TAR construct used in this study.

(B) Chemical structure and numbering system of acetylpromazine.

values, in ppm, respectively): A22H8 (+0.12), A22H3′ (+0.14), U23H6 (+0.16), U23H5 (+0.22), U23H1′ (+0.14), U23H2′ (+0.13), U23H4′ (−0.15), C24H1′ (+0.10), U25H2′ (−0.11), U25H3′ (−0.17), G26H1′ (−0.22), C39H1′ (+0.13), C39H3′ (+0.15), U40H6 (−0.11), U40H5 (−0.10), U40H1′ (−0.18), C41H6 (−0.12), C41H5 (−0.13). All of these chemical-shift changes are observed for nuclei that belong to the three bulged residues U23, C24, U25 and adjacent base pairs (A22, G26, C39, U40, and C41). Even in the presence of a 5-fold excess of acetylpromazine, no noticeable chemical-shift change was detected from nuclei that belong to residues in other regions of TAR. These chemical-shift observations demonstrate that binding of acetylpromazine to TAR is specific to the bulge region. Nonspecific ligand-RNA interactions do not seem to play any role in the interaction between acetylpromazine and TAR.

Besides gathering chemical-shift change data, we also identified a large number of intermolecular NOEs between acetylpromazine and TAR. For example, Figure 3A shows several NOEs between the U40 H1′ proton and acetylpromazine protons in a 3D ^{13}C-edited NOESY-HMQC experiment performed on an RNA sample with only the U residues labeled. Acetylpromazine protons resonate in regions (1.90–3.50 and 6.45–6.95 ppm for aliphatic and aromatic protons, respectively) distinct from those of RNA protons, greatly facilitating identification of intermolecular NOEs between acetylpromazine and TAR. The 51 intermolecular NOEs are shown graphically in Figure 3B and are listed in Table 1. In accord with the chemical-shift data, all RNA resonances involved in intermolecular NOEs are from nuclei in the bulge and flanking base pairs, providing another strong piece of NMR evidence for the very specific binding of acetylpromazine to the bulge region of TAR.

Structure of the Acetylpromazine-TAR Complex

The solution structure of the acetylpromazine-TAR complex was determined with the protocol described in the Experimental Procedures. Structure refinement statistics are summarized in Table 2. Because of the large number of intermolecular NOEs, 51, between acetylpromazine and TAR (Figure 3B), binding of acetylpromazine to the 5′ bulge is very well defined. Figure 4A shows twelve superimposed refined structures of the complex. Except for the poorly defined loop nucleotides (C30–A35), the structures superimpose very well. In Figure 4B, a representative structure is shown, with a ribbon representing the RNA backbone. Two views of the internal bulge region are shown in Figure 5. U23, U25, and benzene ring II of acetylpromazine are placed along the major groove, whereas benzene ring I and the aliphatic moiety of acetylpromazine, together with C24, lie along the minor groove.

The three-member ring of acetylpromazine inserts between base pairs G26-C39 and A22-U40, preventing continuous stacking of the lower and upper stems as observed in structures induced by argininamide or Tat-peptide [8–10]. However, another set of base-stacking interactions is created. U23 continues stacking on A22 in the fashion of an A helix. This is evident by the NOEs from U23 H6 to A22 H2′ and H3′ as well as from U23 H1′ to A22 H2. Benzene ring II of acetylpromazine is stacked on U40. Stacking of U23 on A22 and benzene ring II on U40 arranges the U23 base and benzene ring II such that they look like an extra base pair continuing helical stacking on the A22–U40 base pair. This "pseudo base pair" may contribute to the creation of a deeper minor groove (compared to that of the standard A helix) to accommodate the aliphatic moiety of acetylpromazine. On the major-groove side, U25 stacks on benzene ring II of acetylpromazine. Figure 5B illustrates that benzene ring II is "sandwiched" between the U25 and U40 bases. Benzene ring I, which forms an angle of about 135° with benzene ring II, is positioned below G26. Partial stacking of G26 and benzene ring I is possible.

The aliphatic moiety of acetylpromazine is extended along the minor groove. NOEs from the Hε protons of acetylpromazine to C41 H5 and H1′ protons are observed, indicating that the tail of the aliphatic chain is in close proximity to the G21-C41 base pair. Also in the minor groove, C24 has its base moiety close to the A22-U40 and G21-C41 base pairs. C24 helps to bury the aliphatic chain of acetylpromazine within the minor groove (Figure 5C).

Comparison with Other TAR Structures

Several TAR structures have been reported previously, including a number of NMR structures of free TAR and TAR in the presence of argininamide or Tat-peptide [8–10], an NMR structure of TAR in complex with neomycin B [11], and a crystal structure of the TAR bulge region stabilized by several calcium ions [12]. Free TAR in solution was shown to have U23 stacked on A22, causing helical bending of the molecule. Binding of argininamide, Tat-peptide, or neomycin B to TAR causes conformational changes around the bulge region. In all cases, stacking of U23 on A22 is disrupted, and A22-U40 and G26-C39 base pairs are more or less stacked, resulting in a continuous helix in the RNA stem. Positions of the bulge residues are varied. In argininamide or Tat-peptide

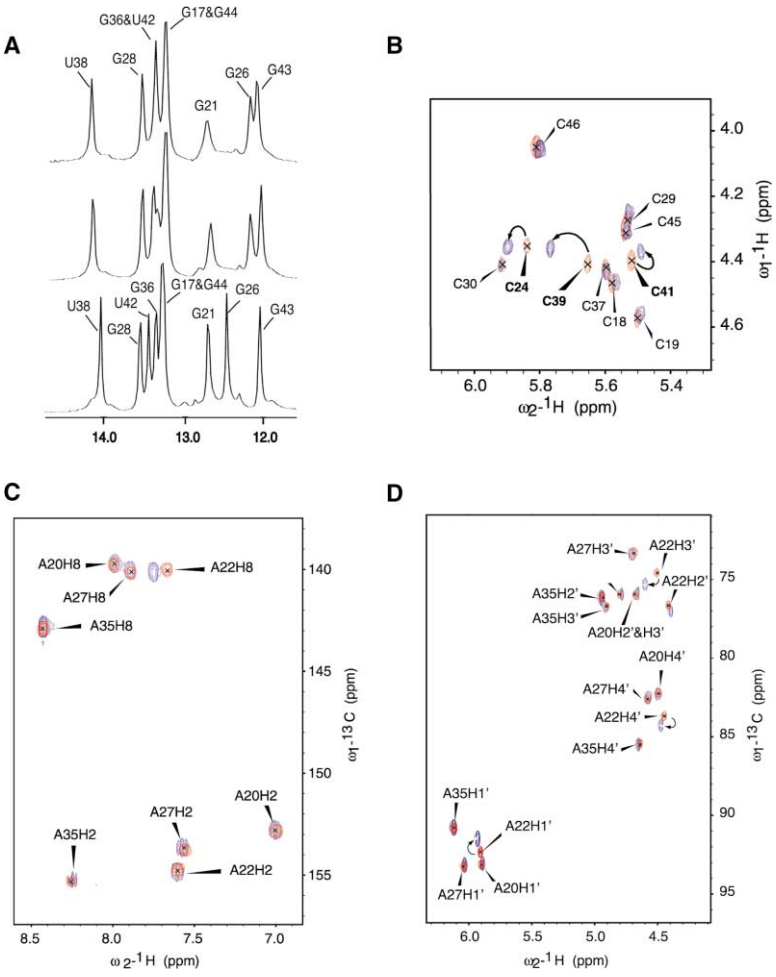

Figure 2. Chemical-Shift Changes of TAR upon Acetylpromazine Binding

(A) 1D imino proton spectra of TAR RNA in the absence and presence of acetylpromazine, as follows: (bottom) free TAR RNA, (middle) TAR-to-acetylpromazine molar ratio of nearly 1 to 1, and (top) TAR-to-acetylpromazine molar ratio of about 1 to 2. The spectra were collected at 10°C. The sample contained about 2 mM TAR RNA in 10 mM sodium phosphate (pH 6.5) and 20 mM NaCl. For the 2D NMR spectra, crosspeaks from the free TAR and TAR-acetylpromazine complex are colored red and blue, respectively. Black arrows indicate notable chemical-shift changes.

(B) 2D HCCH-COSY spectra showing H1′-to-H2′ crosspeaks of a TAR sample with all cytosine residues isotopically labeled.

(C,D) $^{1}H^{13}C$-HSQC spectra of the aromatic and ribose moieties of a TAR sample with all adenine residues isotopically labeled.

bound structures, U23 is in the major groove, C24 is exposed to solvent, and U25 is on the minor groove side; in the neomycin bound conformation, U23 and C24 are both positioned in the minor groove side, and U25 protrudes out of the helix. Whereas binding of argininamide or Tat-peptide occurs on the major groove side, binding of neomycin B is in the minor groove. Clearly, the acetylpromazine bound structure we present here differs from all of the reported TAR structures. Unlike other ligand-induced structures, U23 still stacks on A22 in our structure, which is very similar to free TAR in solution. It was reported that unstacking of U23 on A22 caused a very large upfield shift ($\sim$0.5 ppm) of A22 H2 proton [8–10]. With acetylpromazine, the chemical shift of the A22 H2 proton is virtually unchanged (Figure 2C); α-helical-like interresidue NOEs were observed between U23 and A22. In the acetylpromazine bound structure, stacking between upper and lower stems becomes impossible because of insertion of the three-member ring from the ligand. However, insertion of acetylpromazine benzene ring II between U40 and U25 creates a continuous stack of ten bases (including benzene ring II) involving the non-bulge strand (U40–C46), the ligand, and bulge residue U25. Similar to neomycin B binding, benzene ring I and the aliphatic tail of acetylpromazine are aligned along the minor groove. However, in our complex, the minor groove is not solely defined by the RNA. Instead, benzene ring II is actively involved.

Significance

The acetylpromazine-TAR structure reported here is significant in several respects. First, it justifies the RNA structure-based computational screening procedure we have developed. Second, it suggests possible ways to improve binding specificity and affinity in designing next-generation compounds. Third, our structure clearly differs from the Tat-peptide or argininamide-complexed TAR, suggesting that some variability in the structure of the RNA target may be tolerated. It remains for us to test the extent of initial structure variability that can be tolerated. However, ligands capable of locking TAR into a stable conformation, regardless of similarity to the Tat bound conformation, should prove useful in combating HIV-1 infection. RNA is typically flexible and adopts rather different conformations upon the binding of different ligands. The acetylpromazine-TAR structure not only corroborates this observation but also has fascinating implications for RNA structure-based drug discovery. The discrepancy between the acetylpromazine-induced structure and the Tat-induced structure argues for the feasibility of

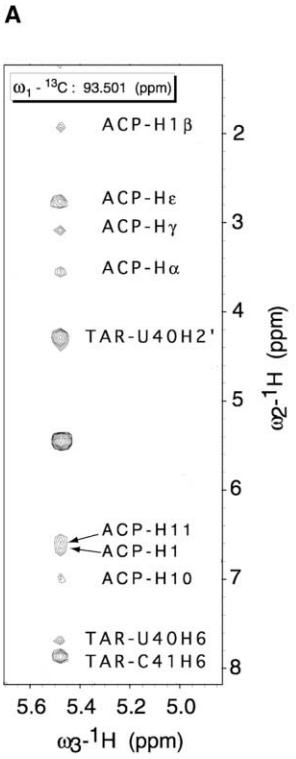

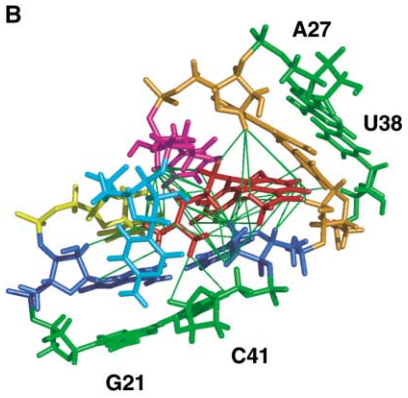

Figure 3. Examples of Intermolecular NOEs between TAR and Acetylpromazine

(A) Shown is a slice at the U40 C1′ chemical shift taken from a ^{13}C-edited 3D NOESY-HMQC spectrum (300 ms mixing time) of a TAR sample with all uracil residues isotopically labeled. Note that the intermolecular NOEs are unambiguously identified because acetylpromazine protons resonate within distinctive chemical-shift ranges without overlapping TAR resonances.

(B) A graphical representation of the 51 intermolecular NOEs that define the interaction between TAR and acetylpromazine. See text for a full list of these NOEs. The coloring schemes are: G21-C41 and A27-U38 base pairs (green), A22-U40 base pair (blue), G26-C39 base pair (gold), U23 (yellow), C24 (cyan), U25 (magenta), and acetylpromazine (red). Each NOE is represented as a thinner green bar connecting the two protons involved.

embarking on a program of structure-based lead compound discovery against a pathogenic RNA even when the conformation of the RNA in complex with its biologically relevant partner has not been determined. This is important because determining the structure of a disease-related RNA molecule can be slow, and some RNA molecules are refractory to structure determination approaches. Finally, although several structures of RNA in complex with small-molecular-weight ligands have been reported, most of these RNA binding ligands fall into one of three categories: amino acid or peptide analog, nucleoside analog, or aminoglycoside. The structure of the acetylpromazine-TAR complex therefore provides new insights into principles of RNA recognition by small organic compounds. The compounds we identified as specific TAR binders may provide a new scaffold for development of novel RNA binding therapeutic agents.

Experimental Procedures

Sample Preparation

Five different samples of the 31 nucleotide TAR were prepared: unlabeled, uniformly ^{13}C,^{15}N-labeled, and type-specifically ^{13}C,^{15}N-labeled at G, A, or C residues, respectively. All samples were prepared by in vitro transcription with T7 RNA polymerase and a synthetic DNA template [13] and purified as described [14]. Acetylpromazine was purchased from Research Diagnostics. Final sample conditions were 1–2 mM RNA in 10 mM sodium phosphate buffer (pH 6.5) and 20 mM sodium chloride. Acetylpromazine was added in about 2-fold excess over RNA.

NMR Spectroscopy

All NMR experiments were performed on Varian Inova 600 MHz spectrometers. Spectra were processed with NMRpipe [15] and analyzed with SPARKY [16]. Homonuclear 2D NOESY spectra in H_2O were collected at 10°C with the SSNOESY pulse sequence [17]. Homonuclear 2D NOESY, DQF-COSY, and TOCSY spectra in D_2O were recorded at 25°C and 35°C. The NOESY spectra were recorded with mixing times of 50, 100, 200, and 300 ms to monitor the NOE

Table 1. Intermolecular NOEs between TAR and Acetylpromazine

Actylpromazine Proton	TAR Proton
H1	G26H1′(w), U40H1′(m), U40H2′(w)
H3	G26H1′(vw), U40H1′(w), U40H4′(m)
H4	G26H1′(vw), C39H2′(m), U40H1′(vw), U40H1′(w), U40H6(w)
H8	C39H2′(w), C39H5(w), C39H6(w), U40H1′(vw), U40H6(m)
H9	U40H1′(vw), U40H6(m)
H10/H11	U25H2′(vw), U25H6(w), U40H1′(s), U40H2′(w)
Hα	U25H2′(m), U25H6(w), G26H1′(w), U40H1′(m)
H1β	C24H2′(vw), U25H2′(w), U25H6(vw), U40H1′(s), U40H2′(w)
Hγ	U25H6(m), U40H1′(m), U40H2′(w), U40H6(vw)
Hϵ	A22H1′(w), A22H2′(vw), U23H1′(m), C24H1′(w), C24H2′(m), U25H2′(w), U25H5(w), U25H6(w), U40H1′(s), U40H2′(m), U40H6(w), C41H1′(w), C41H5(w)
H2β	G26H1′ (vw), U40H1′ (w), U40H2′ (w)

s: strong; m: medium; w: weak; vw: very weak.

Table 2. Restraint and Structure Statistics	
A. Distance and dihedral restraints	
Intranucleotide NOEs	378
Sequential NOEs	179
Medium/long-range NOEs	57
Intermolecular NOEs	51
Total number of NOEs	665
Hydrogen bond restraints	60
Dihedral restraints for sugar puckers	90
Total number of NMR restraints	815
Mean number per residue	25.5
B. Superposition of 12 structures (pairwise rmsd)	
All nucleotides and ACP (Å)	3.17
16–29, 36–46, ACP (Å)	1.23
21–27, 38–41, ACP (Å)	0.82

crosspeak intensity build-ups. One bond-correlated ^{1}H-^{15}N HMQC spectra were obtained at 10°C in H_2O. All heteronuclear experiments in D_2O were performed at 35°C. One-bond ^{1}H-^{13}C correlations were obtained with constant-time HSQC. Adenine H2 proton-to-H8 proton long-range correlations were established by a 2D HCCH-TOCSY experiment. Ribose spin systems were identified by 3D ^{13}C-edited HCCH-COSY and 3D HCCH-TOCSY experiments [18]. Correlations of base and ribose protons were established by 2D HCN experiments. 3D ^{13}C-edited NOESY-HMQC spectra optimized for observation of either base or sugar moieties were recorded with a mixing time of 150 ms. 2D ^{13}C-edited NOESY spectra were collected on the type-specific labeled samples.

NMR-Derived Restraints

Interproton distance restraints between nonexchangeable protons were obtained from the intensities of crosspeaks in the 2D NOE build-up series and the 3D ^{13}C-edited NOESY spectra and were assigned to four categories, as follows: strong (1.8–3.0 Å), medium (1.8–4.0 Å), weak (1.8–5.0 Å), and very weak (1.8–6.0 Å). Distance restraints involving exchangeable protons were assigned to two categories with upper bounds of 4.0 or 6.0 Å, respectively. The very strong NOEs from adenine-H2 to uridine-NH and from cytosine-NH_2 to guanosine-NH within Watson-Crick base pairs were assigned an upper bound of 4.0 Å. All other NOEs in water were assigned an upper bound of 6.0 Å. No intramolecular NOEs within acetylpromazine were used as distance restraints. Hydrogen bond restraints were only imposed on base pairs established by the observation of imino proton resonances and internucleotide NOEs characteristic of base pair formation. These restraints were based on standard base pair geometry of nucleic acids [19] and were given a range of ±0.2 Å. Torsion angle restraints for ribose sugar conformation were based on analysis of the 2D DQF-COSY spectra. Sugars showing a strong H1′-H2′ crosspeak were restrained to C2′-endo. Those with no COSY and TOCSY crosspeaks were interpreted as C3′-endo. All other nucleotides were left unconstrained.

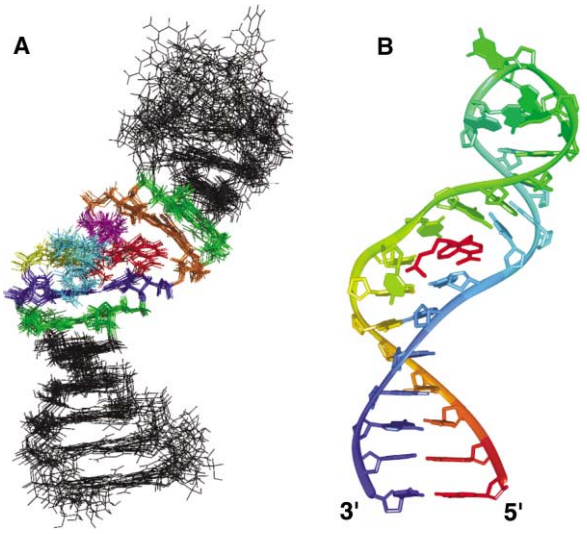

Figure 4. Structures of TAR in Complex with Acetylpromazine

(A) Superposition of the eleven refined structures of the TAR-acetylpromazine complex. The superposition is performed on all residues (including acetylpromazine) of the complex except the poorly defined loop nucleotides (C30–A35). The coloring schemes for residues G21–A27, U38–C41, and acetylpromazine are identical to that in Figure 3B. All other residues are colored black.

(B) One representative structure of the TAR-acetylpromazine complex is shown with color ramping from the 5′ end (red) to the 3′ end (blue) of TAR and with acetylpromazine highlighted in red. The ribbon traces the backbone of TAR.

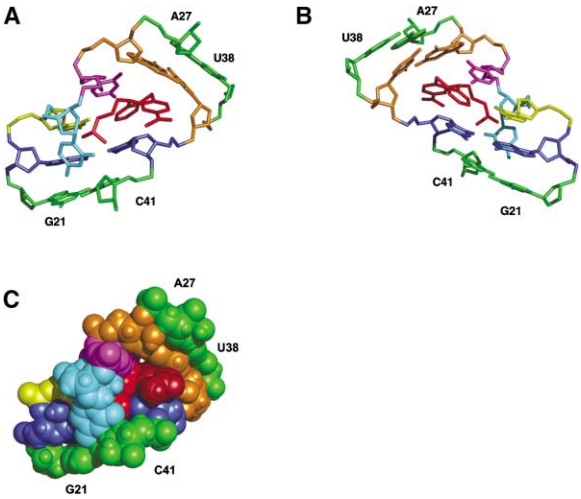

Figure 5. Views of the Bulge Region of the TAR-Acetylpromazine Complex

(A) From the minor groove.

(B) From the major groove (~180° rotation from [A]).

(C) Space-filling representation with the same view as (A). The color scheme is identical to that in Figure 3B except that the aromatic moiety (including the acetyl group) of acetylpromazine is colored darker to distinguish it from the aliphatic moiety, which is embedded in the minor groove.

Structure Determination

Structure refinement was performed with the programs DYANA 1.6 [20] and AMBER 6.0 [21, 22]. DYANA was used to generate 200 random initial structures subject them to simulated annealing in torsion angle space. This was followed by variable target function minimization. The twenty DYANA structures with the lowest target function values and correct chirality (checked with the program CHIRANO, developed by N. Ulyanov at the University of California, San Francisco) were chosen for further refinement via restrained molecular dynamics with AMBER. The 12 structures with the lowest AMBER energy were chosen to represent the final structure ensemble, and these were analyzed with the program CARNAL [21]. All graphical figures were generated with MidasPlus [23].

Acknowledgments

This work was supported by grant AI46967 from the National Institutes of Health. We wish to thank Dr. James R. Williamson for generously giving us the assignments of free TAR and Dr. Nikolai Ulyanov for assistance in using DYANA. We acknowledge use of the Univer-

sity of California, San Francisco Computer Graphics Laboratory supported by National Institutes of Health grant RR01081.

Received: November 27, 2001
Revised: April 10, 2002
Accepted: April 10, 2002

References

1. Lind, K.E., Du, Z., Fujinaga, K., Peterlin, B.M., and James, T.L. (2002). Structure-based computational database screening, in vitro assay, and NMR assessment of compounds that target TAR RNA. Chem. Biol. *9*, 185–193.
2. Filikov, A.V., Mohan, V., Vickers, T.A., Griffey, R.H., Cook, P.D., Abagyan, R.A., and James, T.L. (2000). Identification of ligands for RNA targets via structure-based virtual screening: HIV-1 TAR. J. Comput. Aided Mol. Des. *14*, 593–610.
3. Carroll, R., Peterlin, B.M., and Derse, D. (1992). Inhibition of human immunodeficiency virus type 1 Tat activity by coexpression of heterologous *trans* activators. J. Virol. *66*, 2000–2007.
4. Wimmer, J., Fujinaga, K., Taube, R., Cujec, T.P., Zhu, Y., Peng, J., Price, D.H., and Peterlin, B.M. (1999). Interactions between Tat and TAR and human immunodeficiency virus replication are facilitated by human cyclin T1 but not cyclins T2a or T2b. Virology *255*, 182–189.
5. Hauber, J., Malim, M.H., and Cullen, B.R. (1989). Mutational analysis of the conserved basic domain of human immunodeficiency virus *tat* protein. J. Virol. *63*, 1181–1187.
6. Delling, U., Reid, L.S., Barnett, R.W., Ma, M.Y., Climie, S., Sumner-Smith, M., and Sonenberg, N. (1992). Conserved nucleotides in the TAR RNA stem of human immunodeficiency virus type 1 are critical for Tat binding and trans activation: model for TAR RNA tertiary structure. J. Virol. *66*, 3018–3025.
7. Dingwall, C., Ernberg, I., Gait, M.J., Green, S.M., Heaphy, S., Karn, J., Lowe, A.D., Singh, M., and Skinner, M.A. (1990). HIV-1 Tat protein stimulates transcription by binding to a U-rich bulge in the stem of the TAR RNA structure. EMBO J. *9*, 4145–41153.
8. Puglisi, J.D., Tan, R.Y., Calnan, B.J., Frankel, A.D., and Williamson, J.R. (1992). Conformation of the TAR RNA-arginine complex by NMR spectroscopy. Science *257*, 76–80.
9. Aboul-ela, F., Karn, J., and Varani, G. (1995). The structure of the human immunodeficiency virus type-1 TAR RNA reveals principles of RNA recognition by Tat protein. J. Mol. Biol. *253*, 313–332.
10. Long, K.S., and Crothers, D.M. (1999). Characterization of the solution conformations of unbound and Tat peptide-bound forms of HIV-1 TAR RNA. Biochemistry *38*, 10059–10069.
11. Faber, C., Sticht, H., Schweimer, K., and Rösch, P. (2000). Structural rearrangements of HIV-1 Tat-responsive RNA upon binding of neomycin B. J. Biol. Chem. *275*, 20660–20666.
12. Ippolito, J.A., and Steitz, T.A. (1998). A 1.3-Å resolution crystal structure of the HIV-1 trans-activation response region RNA stem reveals a metal ion-dependent bulge conformation. Proc. Natl. Acad. Sci. USA *95*, 9819–9824.
13. Milligan, J.F., and Uhlenbeck, O.C. (1989). Synthesis of small RNAs using T7 RNA polymerase. In Methods in Enzymology, J.E. Dahlberg and J.N. Abelson, eds. (New York: Academic Press), pp. 51–62.
14. Du, Z., Giedroc, D.P., and Hoffman, D.W. (1996). Structure of the autoregulatory pseudoknot within the gene 32 messenger RNA of bacteriophages T2 and T6: a model for a possible family of structurally related RNA pseudoknots. Biochemistry *35*, 4187–4198.
15. Delaglio, F., Grzesiek, S., Vuister, G.W., Zhu, G., Pfeifer, J., and Bax, A. (1995). NMRPipe: a multidimensional spectral processing system based on UNIX pipes. J. Biomolec. NMR *6*, 277–293.
16. Goddard, T.D., and Kneller, D.G. (1998). SPARKY 3.0, University of California, San Francisco.
17. Smallcombe, S.H. (1993). Solvent suppression with symmetrically-shifted pulses. J. Am. Chem. Soc. *115*, 4776–4785.
18. Nikonowicz, E.P., and Pardi, A. (1993). An efficient procedure for assignment of the proton, carbon and nitrogen resonances in $^{13}C/^{15}N$ labeled nucleic acids. J. Mol. Biol. *232*, 1141–1156.
19. Saenger, W. (1984). Principles of Nucleic Acid Structure. (New York: Springer).
20. Güntert, P., Mumenthaler, C., and Wüthrich, K. (1997). Torsion angle dynamics for NMR structure calculation with the new program DYANA. J. Mol. Biol. *273*, 283–298.
21. Pearlman, D.A., Case, D.A., Caldwell, J., Ross, W.S., Cheatham III, T.E., Ferguson, D.N., Seibel, G.L., Singh, U.C., Weiner, P.K., and Kollman, P.A. (1995). AMBER 4.1. University of California, San Francisco.
22. Cornell, W., Cieplak, P., Bayly, C.I., Gould, I.R., Merz, K.M., Ferguson, D.M., Spellmeyer, D.C, Fox, T., Caldwell, J.W., and Kollman, P.A. (1996). A second generation force field for the simulation of proteins, nucleic acids, and organic molecules. J. Am. Chem. Soc. *117*, 5179–5197.
23. Gallo, K., Huang, C., Ferrin, T.E., and Langridge, R. (1989). Molecular interactive display and simulation (MIDASplus). University of California, San Francisco.

Accession Numbers

Coordinates have been deposited with the Protein Data Bank with accession number 1LVJ.